

Colossal Magnetoresistance in the Perovskite Manganites

Akilan Palanisami

May 2, 2000

Abstract

The basic phenomenology $Re_{1-x}A_xMnO_3$, where Re is a rare earth metal and A is a divalent alkali, is studied as a function of doping. In particular, the ferromagnetic ground state found at $x \simeq 0.3$ and the metal insulator transition which occurs there is studied as a function of temperature and field. An overview of double exchange theory and localization due to polarons is also given.

1 Introduction

In the past decade, interest in magnetoresistive materials has exploded, due mainly to their use in the computer industry. More recently, it has been found that certain transition metal oxides (manganite perovskites) also have a large magnetoresistance (MR). This has been dubbed colossal magnetoresistance (CMR), mainly to differentiate it from giant magnetoresistance. The early physics of CMR invoked a spin scattering argument (double exchange) to explain the large MR. This theory has lately been outmoded by new theories using electron-phonon interactions as the source of electron localization. However a complete theory of CMR has yet to be accepted. This paper will focus on CMR in the perovskite manganites¹ and will first review some of their basic properties. Next, the physics of double exchange and its failure in these materials will be discussed. Some new explanations involving electron-phonon coupling will then be looked at. Finally, recent investigations probing the phase transition itself for differently doped manganites will be reviewed.

2 Basic Phenomenology

The most commonly studied perovskite manganites have the chemical structure $Re_{1-x}A_xMnO_3$, where Re is a rare earth metal (La or Pr for instance) and A is a divalent alkali (such as Ca or Sr) (see figure 1). The important electrons in this system lie in the 3d shell of the Mn. Ca and Sr act as hole dopants here, so that $(4-x)$ electrons lie in the 3d shell of the Mn. These electrons will have all their spins aligned, giving the Mn atom a net moment. Changing the doping brings about a variety of different phases, as shown in figure 2 for $La_{0.75}Ca_{0.25}MnO_3$. At $x=0$, the material is always insulating and is paramagnetic at higher temperatures, while anti-ferromagnetic ordering sets in at lower temperatures. The anti-ferromagnetic ordering is as follows, all of the moments in the plane perpendicular to the c-axis lie parallel to one another, but the orientation of these spins flip from plane to plane (this is designated as CAF, for canted anti-ferromagnet, in the diagram). As the doping is increased, the anti-ferromagnetic order changes in a non-trivial process to ferromagnetic order. The medium is still insulating at all temperatures here (FI, for ferromagnetic insulator, in the diagram). For $0.07 < x < 0.17$, $La_{0.75}Ca_{0.25}MnO_3$ also has a charge ordered phase in addition to the magnetic order described above (denoted CO in the diagram). By charge order, a periodic change of valence electrons in the Mn is meant. For $x=x_{MI}$, the ground state now becomes metallic in addition to being ferromagnetic (FM in the diagram). CMR refers to the metal insulator transition that can occur when the material has a ferromagnetic metallic ground state. If the temperature is raised just above the transition and a magnetic field is

¹CMR is also seen in the pyrochlores (e.g. $Tl_2Mn_2O_7$), the spinels (ACr_2Ch_4 , where A is tetrahedrally coordinated cation [Fe, Cu, or Cd for instance], and Ch is a chalcogen [S, Se, Te]), and some ferromagnetic semiconductors.

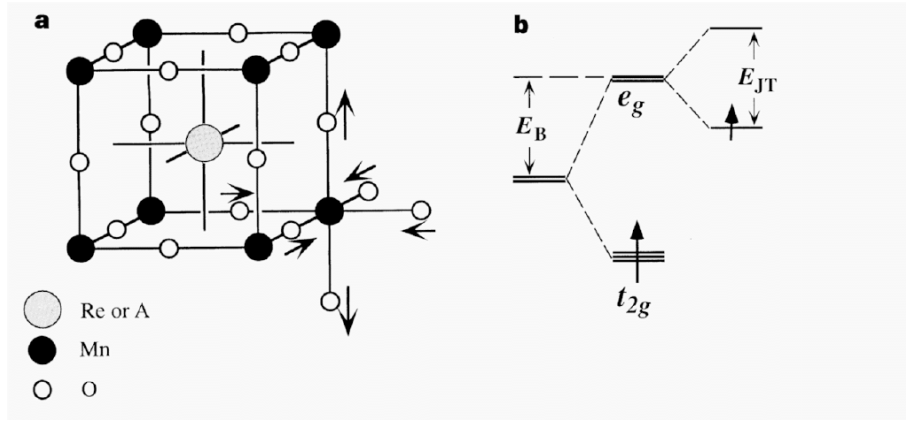


Figure 1: Crystal structure and electronic structure of perovskite manganite a) Basic perovskite structure, with arrows indicating Jahn-Teller distortion b) Schematic energy levels of Mn ion. The central portion is for an undistorted lattice. The d shell splits into low lying t_{2g} triplet, and higher lying e_g doublet (two fold degenerate in the ideal crystal). The right hand part of the figure indicates the distortion of the levels when the e_g level is singly occupied (Jahn-Teller distortion). The left side of the figure shows if the e_g level is unoccupied, a breathing distortion may occur, lowering the level of the unoccupied e_g doublet by an amount E_B relative to the ideal structure.[1]

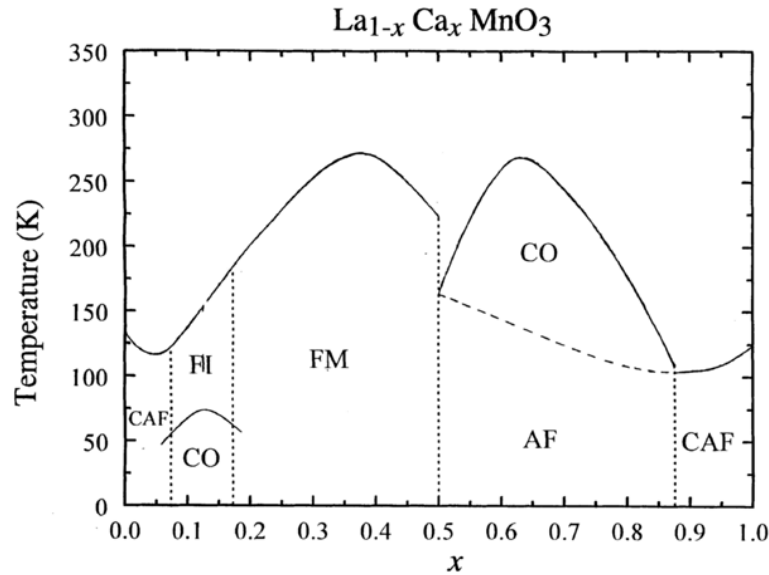


Figure 2: Phase diagram of $La_{1-x}Ca_xMnO_3$ showing magnetic and structural phases. The phases include charge ordered (CO), canted antiferromagnet (CAF), ferromagnetic metal (FM), and ferromagnetic insulator (FI) as described in the text. The unlabelled region of the phase diagram represents a paramagnetic insulating phase[1]

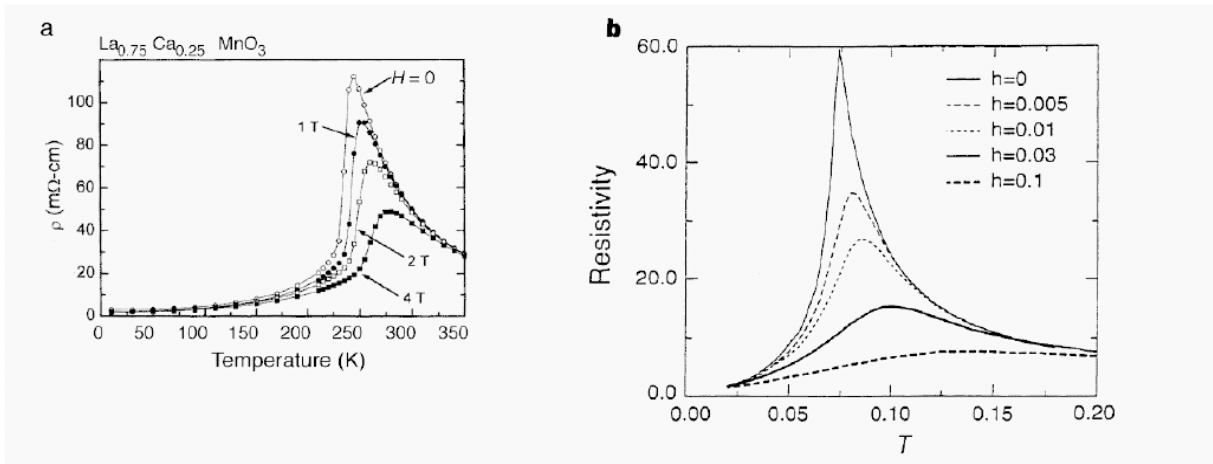


Figure 3: Measured and calculated resistivity of $La_{0.75}Ca_{0.25}MnO_3$ a) Measured resistivity at different magnetic fields[2]. b) Calculated resistance vs temperature[4]

applied, the system will be driven into the ferromagnetic metallic state (figure 3), hence the name colossal magnetoresistance. For $x > 0.75$, the material is once again insulating, with various anti-ferromagnetic and charge ordered phases. I should note that the anti-ferromagnetic order in these regions are not the same as described in the low doped material (for more information, see the review article by V.M. Lotkev and Yu.G. Pogorelov [3]). The remainder of this paper will focus on the CMR transition at roughly $x=0.3$ doping.

3 Double Exchange Theory for CMR

This theory, originally proposed by Zener [5], was first applied to the manganites by K. Kubo and N. Ohata [6] to account for the simultaneous appearance of ferromagnetic order and metallic behaviour. To explain double exchange, a little must first be said about the electronic structure about the Mn site. In an ideal lattice, the 3d orbital will split into two states, a t_{2g} triplet and an e_g doublet (see figure 1). This is due to the crystal field created by the cubic symmetry surrounding the Mn site. The e_g doublet lies 2-4ev above the t_{2g} triplet in energy. The coulomb repulsion forces each electron to lie on a separate level, and the Hund's rule coupling is strong enough to ensure that all 3d electrons on the Mn site are ferromagnetically aligned. Three electrons go to fill the lower lying t_{2g} states, forming an inert core spin of $S=3/2$. The remaining electrons lie in a superposition of the e_g states. These electrons may move through the lattice subject to the constraint that the hopping electron always has its spin aligned with its host's core spin. The hopping from Mn to Mn is mediated by the O^{2-} between them. This hopping action is termed double exchange. As temperature is lowered and spin fluctuations decrease, the crystal lowers its energy by ferromagnetically aligning the Mn core spins, allowing the e_g

electrons to gain kinetic energy and move about the crystal.

The hopping transfer integral calculated from such a theory is a very sensitive function of the Mn-O-Mn bond angle, deviations from 180 degrees resulting in a much reduced hopping probability. This agrees with experimental evidence, where different divalent dopants with different atomic radii bring about large changes in the T_c . Dopants with small atomic radii cause a buckling in the Mn-O-Mn bond angle, decreasing the single electron bandwidth and consequently reducing the T_c . The effect of a dopant's size on the transport properties can be loosely described using a tolerance factor, which describes the degree of deviation of the unit cell from cubic. A tolerance factor of 1 refers to a cubic cell.

Tolerance factor is not the sole determinant of the hopping transfer integral, as lattice distortions are caused by several factors. Different ion radii at different sites can cause local distortion between the cells. As the dopants are randomly placed in the material, this distortion will be of a statistical nature. Also, dopants will have differing amounts of core charge which bring about small coulomb fields which must be compensated for. This is often done by distortions of the oxygen octohedra which surround the Mn site, as they are the most flexible structure in the lattice. These above factors, in addition to the tolerance factor, will change the Mn-O-Mn bond angle, modifying the transfer integral. Also important is the length between neighboring Mn. Known as magnetostriction, it refers to a change of unit cell dimensions as a material undergoes a magnetic transition (this effect is responsible for the hum in transformers). The dimensions of a unit cell can be perturbed using external pressure, and experiments have been done which drive a CMR manganite from insulator to metal by fixing temperature and varying only pressure[7].

4 Failure of the Double Exchange Model

Double exchange theory was initially invoked to provide a link between the observed change in resistance and magnetization with the idea that at high temperature, spin disorder would scatter electrons, while at low temperature, the spins would become more ordered and such scattering would be inhibited. The problem is, even with maximum spin disorder, the resulting electron scatter is not very large[8], as only a negligible fraction of carriers are localized. Additional problems become apparent when the double exchange model is actually solved when including the spin fluctuations[9]. Such a calculation (see figure 4) gives a number of discrepancies, in addition to the one mentioned. Looking at figure 4, the solution predicts an increase in resistivity as T decreases just below T_c or in a field. Comparing this to real data (inset in figure 4), it is seen the resistivity actually decreases quite sharply immediately below T_c . It is interesting to note that the resistivity has the proper behavior with temperature when spin fluctuations are ignored in the calculation. Above T_c , the model has the correct qualitative behavior, however the resistance is

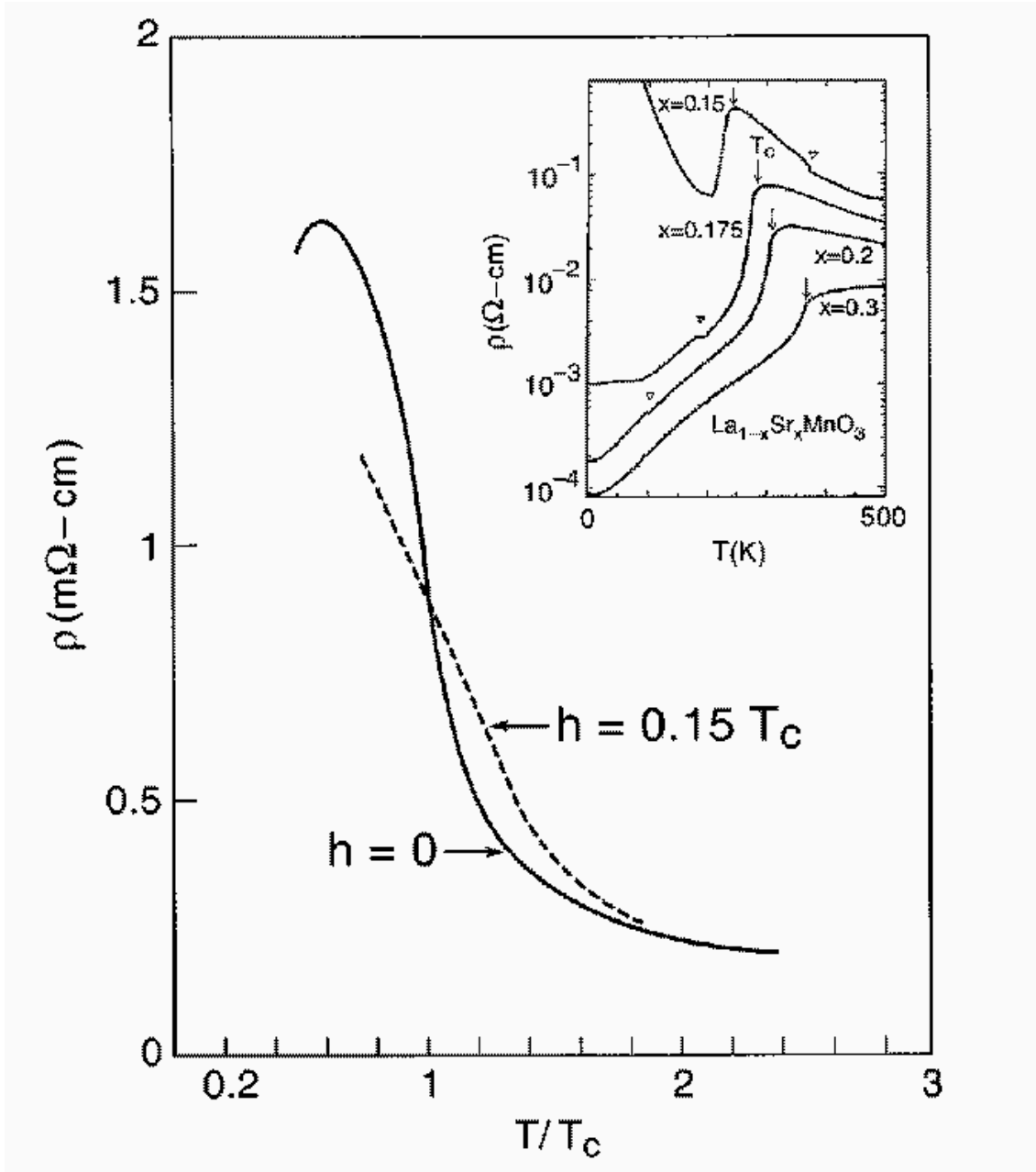


Figure 4: Resistivity calculated from double exchange model[9]. The solid line is the resistivity in zero field. The dashed line is in a field of $0.15T_c$. The inset is unpublished data from Y. Tokura.

off by several orders of magnitude. In addition, the doping dependence of the model is too slow, and its behavior in a field is incorrect. These erroneous results stem from the small effects of spin scattering off of magnetic fluctuations, resulting in a fermi liquid like picture of weakly scattered bandlike electrons.

5 Electron Phonon Coupling

5.1 As a Theoretical Fix

It is obvious from the above discussion that additional physics is necessary. One such mechanism can be found in electron-phonon coupling, which couple instantaneous deviations of atoms from their ideal positions to the instantaneous deviation of electron configurations from their ideal configuration. One important mode is a ‘breathing’ distortion of the O_6 octohedra about a particular Mn atom (see figure 1). This distortion modulates the energy of the e_g orbital. Two other linearly independent, even parity uniaxial volume preserving modes (Jahn-Teller distortions) result in a splitting of the e_g doublet, resulting in a preferred occupancy of one orbital over the other (see figure 1). It can be seen that the Jahn-Teller distortion will lower the energy when the e_g orbital is singly occupied. Thus an electron in a Mn orbital will cause a lattice deformation, lowering its energy. Such a ‘self trapped’ electron is called a polaron and may be the cause of the localization. Theories using polarons have been produced and can give good results[4] (see figure 3).

5.2 Experimental Evidence for Polarons

In undoped $LaMnO_3$, every unit cell has an e_g electron, producing a Jahn-Teller distortion in every cell in the lattice. This causes a deviation from the ideal crystal structure, some Mn-O bonds shrinking and others growing. This distortion occurs in a periodic fashion and can be measured using Bragg scattering. Actual data from such measurements indicate a distortion of $\sim 0.2A$ (about 10%) in the Mn-O bond length, implying a strong Jahn-Teller coupling. As doping is increased, the Jahn-Teller distortion is suppressed, but theoretical models still predict a non-trivial distortion for $x \sim 0.3$ in the $T > T_c$ insulating phase[4].

Evidence for polarons has also been seen in extended X-ray absorption fine structure (see figure 5). The figure plots the root mean square of the deviation of the Mn-O bond length as a function of temperature for different doping. The open square correspond to undoped $LaMnO_3$, which has large variability in its Mn-O bond length, as expected from the discussion in the previous paragraph. The open diamonds along the bottom refer to $CaMnO_3$, where no Jahn-Teller distortion should occur, as the e_g levels are empty. For intermediate dopings, the Mn-O bond length is seen to jump with temperature, indicating the rapid onset of Jahn Teller distortions.

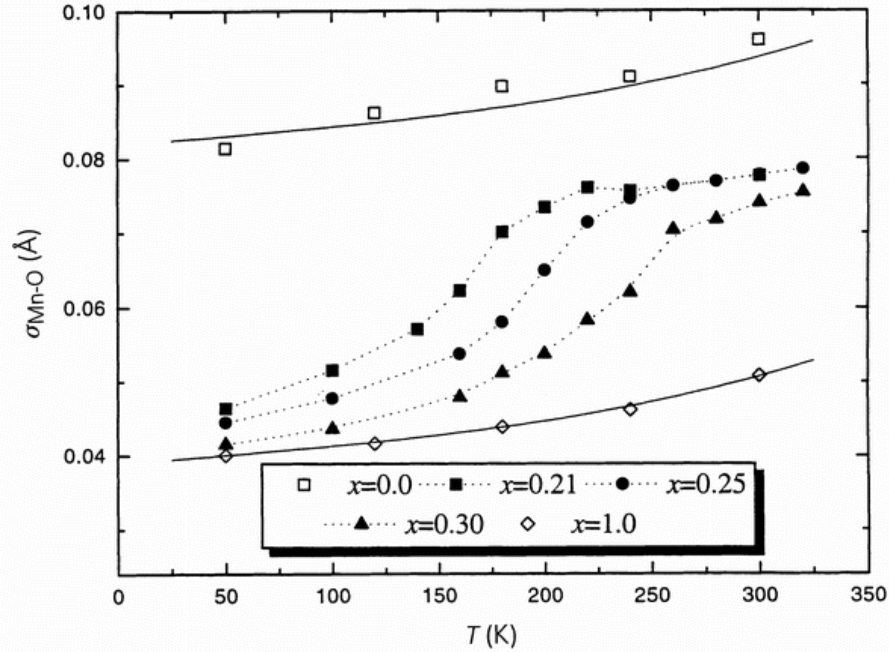


Figure 5: Temperature dependence of variance of Mn-O bond length for $La_{1-x}Ca_xMnO_3$ at various concentrations of x . [10]

A striking example of dynamic electron-lattice coupling is seen in the colossal isotope effect [11]. Here, the T_c is measured before and after exchanging O^{18} with O^{16} (95% full exchange). This exchange resulted in the lowering of the T_c of $La_{0.8}Ca_{0.2}MnO_3$ from 210K to ~ 190 K. This is in contrast to the absence of observed T_c shift in the itinerant ferromagnet $SrRuO_3$, where an 80% exchange of O^{18} with O^{16} was executed. The large T_c shift with oxygen mass has not yet been explained by theory, but is most likely coupled to the magnetism via the modification of the Jahn Teller polaron mass. This effect is a very clear indication that this transition in the perovskite manganites is not purely electronic in nature but must include dynamic lattice effects.

Further evidence for polaronic activity is given by Hall effect measurements, which give a negative carrier charge for $T > T_c$ in thin films of $(La_{1-y}Gd_y)_{0.67}Ca_{0.33}MnO_3$ [12] (Gd was used to lower the T_c). This is unexpected as the material is ostensibly hole doped with 1/3 Ca. It is argued in the paper that this anomalous carrier sign results from interference effects of nearest neighbor loops, which are treated as Aharonov-Bohm loops, along which carriers hop. When these loops contain an odd number of links, an anomalous carrier charge sign can occur for polaronic hopping conduction [13]. Hall effect measurements were also carried out on $La_{1-x}Ca_xMnO_3$ films both above and below T_c [14]. Near T_c , the carrier charge switched from positive to negative, in agreement with the previous experiment. The authors also report the intriguing result that the Hall mobility

$B^{-1} \tan \theta$, where B is the magnetic induction and θ is the hall angle, is field independent near T_c . This implies that the CMR effect is due to a field induced increase in the number of carriers, in contradiction to the double exchange picture of spin scattering, as the cause of increased resistance.

Despite the above evidence (as well as additional optical and thermopower evidence [15]), some feel the case for polarons as the critically important physics in the CMR effect not been completely determined [3]. A major argument for this lies in the ferromagnetic semiconductors in which CMR is seen, but for which there is no evidence of polarons. Another point is the uncertainty in the thermal stability of the polarons at T_c . Finally, other sources of lattice distortion may also be important in the electron localization, such as thermal rotations of the O^6 octohedra.

6 Nature of the Metal Insulator Transition

The nature of the CMR transition as a function of dopant type has been the subject of some controversy over the past few years. Many of the manganites appear to have a continuous phase transition with temperature ($La_{1-x}Sr_xMnO_3$ for instance). For other materials, the issue has been a bit more clouded. Noise measurements are an elegant and relatively simple technique with which to investigate the properties of a phase transition. The following work [16] used noise measurements to investigate the critical behavior of polycrystalline $La_{5/8-x}Pr_xCa_{3/8}MnO_3$ with $x=0.35$ (figure 6). This material is observed to have a smooth magnetization dependence with temperature at T_c (usually indicative of a continuous phase transition) and blatant thermal hysteresis (indicative of a 1st order phase transition). This material also has a very sharp change in resistivity at T_c . Noise measurements of this material are also shown in figure 6. The noise here is measured as $(S_V/V^2)fv_s$ at 10 Hz where V is the sample voltage, f is the frequency of the noise, v_s is the sample volume, and S_V (noise power) is defined as the cosine transform of the voltage-voltage autocorrelation function.

$$S_V(f) = 4 \int_0^\infty (\langle V(\tau)V(0) \rangle - \langle V \rangle^2) \cos(2\pi f\tau) d\tau \quad (1)$$

So figure 6b is basically a normalized measure of the 10Hz noise as a function of temperature. Qualitatively, the normalized noise power is seen to spike at T_c and then slowly increase with temperature². Spikes in noise at phase transitions are not by themselves unusual. Increases in noise of 1-2 orders of magnitude are not uncommon in homogeneous magnetic materials [18]. However, the noise here is seen to increase 4 orders of magnitude at the transition. Such a diverging noise power is consistent with a percolating metal insulator transition [19]. The picture

²It is interesting to note that, even away from the transition, the noise is quite large. For comparison, typical values of $(S_V/V^2)fv_s$ range from $10^{-21} - 10^{-25} cm^3$ in disordered metals and $10^{-18} - 10^{-21} cm^3$ in semiconductors[17]. In fact, the authors claim this system displays the largest normalized 1/f noise power recorded in a condensed matter system to date.

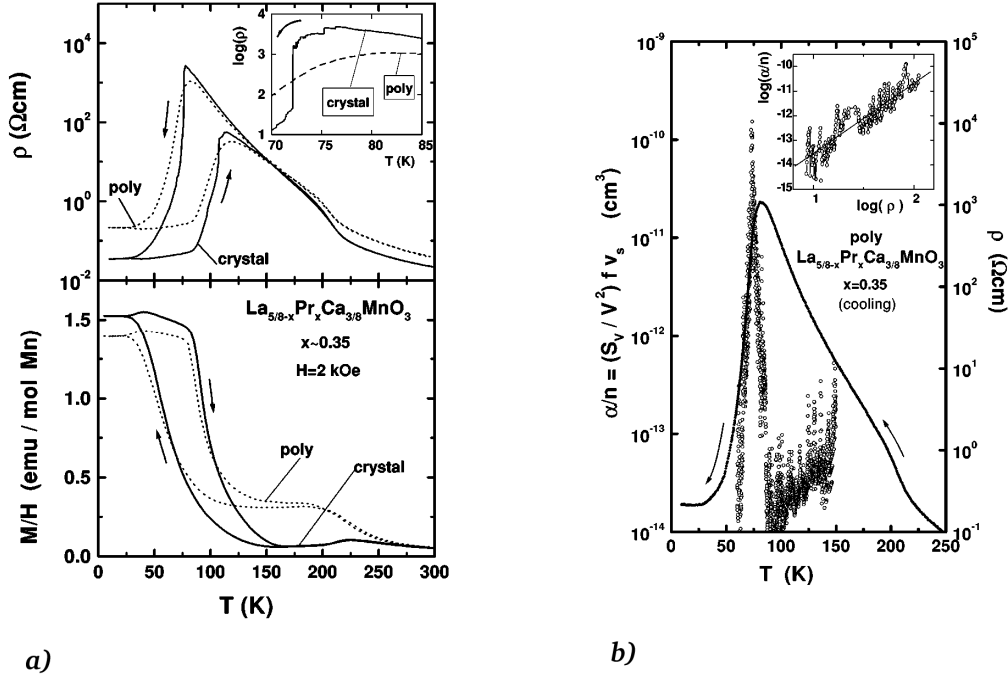


Figure 6: **a)** Upper panel: temperature dependence of the resistivity of $La_{5/8-x}Pr_xCa_{3/8}MnO_3$ ($x=0.35$) (dashed line-polycrystalline sample, solid line-single crystal sample). The inset is a blowup of $\rho(T)$ for cooling near T_c . Lower panel: temperature dependence of the magnetic susceptibility for the same samples measured at $H=2$ kOe. The arrows indicate the direction of the temperature change. **b)** The temperature dependence of the resistivity and the normalized spectral density of the $1/f$ noise, α/n , for the polycrystalline sample $La_{5/8-x}Pr_xCa_{3/8}MnO_3$ ($x=0.35$) for cooling. The noise was measured at $f=10$ Hz; the background noise signal with no current through the sample has been subtracted. The inset shows the scaling dependence of the normalized magnitude of the $1/f$ noise versus ρ in the interval $T=61\text{K}-73\text{K}$ (below $T_c=73\text{K}$). The solid line corresponds to the power-law fit $\alpha/n \propto \rho^{2.9}$. [16]

is as follows, as temperature is reduced in the insulating phase, ferromagnetic conducting regions will progressively appear until a percolating conduction path forms. Fluctuations in this percolating path are what lead to the large increase in noise at the critical temperature. Such a hypothesis is consistent with the observation of ferromagnetic regions at $T \gg T_c$ [20]. Continuing this hypothesis, a large percolation cluster should appear for $T < T_c$, which is consistent with the observation that the maximum $d\rho/dt$ occurs at the same temperature as when the noise diverges. The measured T_c is also lower than the temperature of the maximum ρ , which is expected for a percolation transition.

The diverging nature of the noise at T_c allows scaling to be done on the metallic side of the phase transition. The expected scaling behavior of ρ and S_V/V^2 is [19]

$$\frac{S_V}{V^2} \propto (p - p_c)^{-k} \quad (2)$$

$$\rho \propto (p - p_c)^{-t} \quad (3)$$

where p is the concentration of the metallic phase, p_c is the critical concentration, k is the critical exponent for the noise, and t is the critical exponent for the resistivity. Combining the two gives

$$\frac{S_V}{V^2} \propto \rho^{\frac{k}{t}} \quad (4)$$

Fitting this scaling relation with the data gives the ratio $k/t = 2.9 \pm 0.5$ (see inset figure 6b). This matches well with the $k/t = 3$ measured in mixed powder system of conducting and insulating materials [21]. Theoretical models of conducting blobs in an insulating background give a $k/t = 2.4$ (the inverted random void model). One should note that these numbers are significantly larger than predictions given by discrete random models, which give $k/t \simeq 0.5 - 0.8$, although the value of t is nearly the same in both models ($t \simeq 1.9$).

The values of k and t were obtained from the data by approximating the magnetization as a linear function of $(T - T_c)$ and using $M \propto (p - p_c)$. This allows the substitution of $(T - T_c)$, which is known, for $(p - p_c)$, which is unknown. Using this substitution in the above scaling relations gives critical exponents of $t = 2 \pm 0.3$ and $k = 5.9 \pm 1.5$, which is consistent with the inverted random void model of continuum percolation.

Single crystal samples of $La_{5/8-x}Pr_xCa_{3/8}MnO_3$ were also studied. While having the same gross features as the polycrystalline sample, the change in ρ at T_c was much more abrupt, with large step like jumps apparent. The size of these jumps indicates that the ferromagnetic regions are much larger than in the polycrystalline case. In addition the divergence in the noise at T_c is much larger, spanning more than 6 orders of magnitude. The percolation model breaks down in this regime as the experiment is now probing an inhomogeneous system at a length scale smaller than the percolation correlation length.

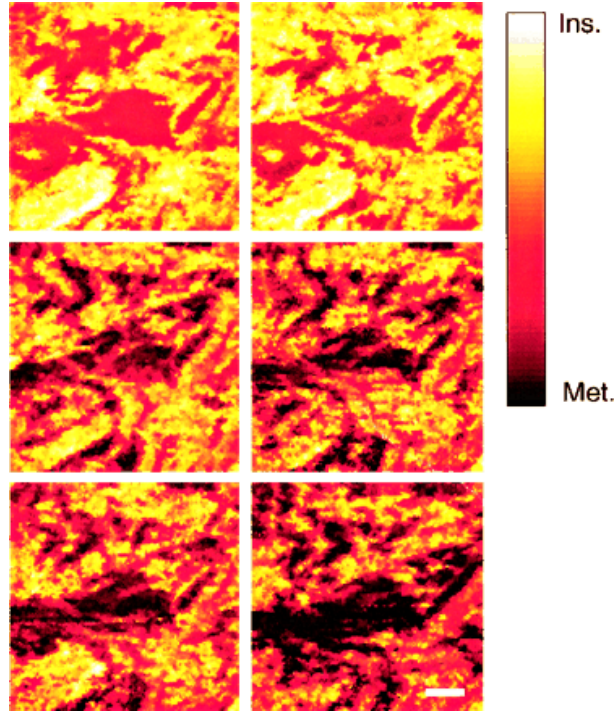


Figure 7: Generic spectroscopic images ($0.61\mu\text{m}$ by $0.61\mu\text{m}$; scale bar 100nm) of the local electronic structure of $\text{La}_{1-x}\text{Ca}_x\text{MnO}_3$ ($x \simeq 0.3$) taken just below T_c in magnetic fields of 0, 0.3, 1.3, 5 and 9 T (from left to right and top to bottom). Parts of the surface are insulating (light colors), whereas others are metallic (dark colors) or in an intermediate state. The color represents the slope of the local I-V spectrum at a bias of 3V. The data were taken on a thin film sample. [22]

This inhomogeneous state has also been clearly seen in STM studies (figure 7)[22]. Note that, even in large fields, parts of the sample remain paramagnetic. The authors also find insulating regions far below T_c .

Knowing that the transition is percolative (at least in some of the manganites), one would expect, if the transition is locally 1st order, to see two state systems in the resistance of a sample near the critically point as single domains lying along percolating pathways flipped between the metallic and insulating states. This was recently seen[23] in $\text{La}_{1-0.33}\text{Ca}_{0.33}\text{MnO}_3$ (see figure 8). Furthermore, these two state systems could be perturbed by tuning the temperature and magnetic field, allowing the authors to probe an individual domain and estimate both its size and the latent heat of its phase transition. $\text{La}_{1-0.33}\text{Sr}_{0.33}\text{MnO}_3$ displayed no such two state systems. In fact, its noise magnitude rivaled that of an ordinary metal, suggesting that its phase transition is locally continuous.

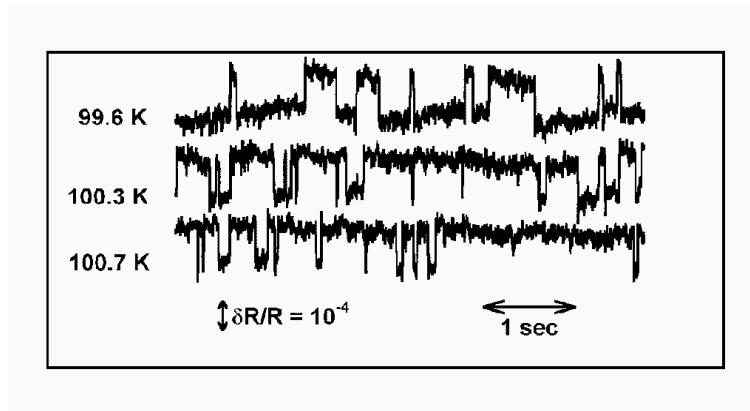


Figure 8: Some time traces exhibiting discrete fluctuators in the $(La_{1-0.33}Ca_{0.33}MnO_3)$ film at different T. The high R state is favored at higher T. [23]

7 Summary

The transition metal oxides present a host of exotic properties which have yet to be fully understood. This is evidenced by the ferromagnetic metallic behavior seen in the oxides discussed here and the high temperature superconducting behavior seen in the copper oxides. Fermi liquid theory, valid in many metals, is obviously inappropriate for these materials. Studying the CMR transition of the manganites provides one venue with which to study this class of materials. It is evident, however, that CMR is one facet of a many body phenomena, as is seen by the associated charge ordering, magnetic field induced structural transitions, and colossal isotope effect. The manganite perovskites provide, through the aforementioned phenomena, a unique opportunity to study the poorly understood physics of systems with high densities of electrons strongly coupled to phonons, as well as the interplay between lattice deformations and macroscopic properties.

References

- [1] A.J. Millis *Nature*, **392**:147, 1998.
- [2] P. Schiffer, A.P. Ramirez, W. Bao, S-W. Cheong *Phys. Rev. Lett.*, **75**:3336, 1995.
- [3] V.M. Lotkev and Yu.G. Pogorelov *Low Temp. Phys.*, **26**:171, 2000.
- [4] A.J. Millis, R. Mueller, B.I. Shraiman *Phys. Rev. B*, **54**:5404, 1996.
- [5] C. Zener *Phys. Rev.*, **82**:403, 1951.
- [6] K. Kubo and N. Ohata *J. Phys. Soc. Jpn.*, **33**:21, 1972.
- [7] J.M.D. Coey, M. Viret and S. von Molnar *Adv. in Phys.*, **48**:167, 1999.
- [8] Q. Li, J. Zang, A.R. Bishop and C.M. Soukoulis *Phys. Rev. B*, **56**:4541, 1997.
- [9] A.J. Millis P.B Littlewood and B.I. Shraiman *Phys. Rev. Lett.*, **74**:5144, 1995.
- [10] C.H. Booth, F. Bridges, G.H. Kwei, J.M. Lawrence, A.L. Cornelius, J.J. Neumeier *Phys. Rev. Lett.*, **80**:853, 1998.
- [11] G. Zhao, K. Conder, H. Keller and K.A. Muller *Nature*, **381**:676, 1996.
- [12] M. Jaime, H.T. Hardner, M.B. Salamon, M. Rubinstein, P. Dorsey and D. Emin *Phys. Rev. Lett*, **78**:951, 1997.
- [13] D. Emin and T. Holstein *Ann. Phys.*, **53**:439, 1969.
- [14] P. Matl, N.P. Ong, Y.F. Yan, Y.Q. Li, D. Studebaker, T. Baum and G. Doubinina *Phys. Rev. B* , **57**:10248, 1998.
- [15] A.P. Ramirez *J. Phys.: Condens. Matter*, **9**:8171, 1997.
- [16] V. Podzorov, M. Uehara, M.E. Gershenson, T.Y. Koo and S-W. Cheong *Phys. Rev. B*, **61**:3784, 2000.
- [17] Sh. Kogan *Electronic Noise and Fluctuations in Solids* (Cambridge University Press, Cambridge, 1998).
- [18] H.T. Hardner, M.B. Weissman, M. Jaime, R.Ej Treece, P.C. Dorsey, J.S. Horwitz and D.B. Chrisey *J. Appl. Phys*, **81**:272 ,1997.
- [19] A.-M. S. Tremblay, S. Feng and P. Breton *Phys. Rev. B*, **33**:2077, 1986.
- [20] J.M. de Teresa, M.R. Ibarra, P.A. Algarabel, C. Ritten, C. Marquina, J. Blasco, J. Garcia, A. del Moral and Z. Arnold *Nature*, **386**:256, 1997.

- [21] D.A. Rudman, J.J. Calabrese and J.C. Garland *Phys. Rev. B*, **33**:1456, 1986.
- [22] M. Fath, S. Freisem, A.A. Menovsky, Y. Tomioka, J. Aarts and J.A. Mydosh *Science*, **285**:1540, 1999.
- [23] R.D. Merithew, M.B. Weissman, F.M. Hess, P. Spradling, E.R. Nowak, J. O'Donnell, J.N. Eckstein, Y. Tokura and Y. Tomioka *Phys. Rev. Lett.* **84**:3442, 2000.